

# VCP/p97 controls signals of the ERK1/2 pathway transmitted via the Shoc2 scaffolding complex: novel insights into IBMPFD pathology

Hyeln Jang<sup>a,†</sup>, Eun Ryoung Jang<sup>a,†</sup>, Patricia G. Wilson<sup>a</sup>, Daniel Anderson<sup>b</sup>, and Emilia Galperin<sup>a,\*</sup>

<sup>a</sup>Department of Molecular and Cellular Biochemistry, University of Kentucky, Lexington, KY 40536;

<sup>b</sup>Cleave Biosciences, Burlingame, CA 94010

**ABSTRACT** Valosin-containing protein (VCP), also named p97, is an essential hexameric AAA+ ATPase with diverse functions in the ubiquitin system. Here we demonstrate that VCP is critical in controlling signals transmitted via the essential Shoc2-ERK1/2 signaling axis. The ATPase activity of VCP modulates the stoichiometry of HUWE1 in the Shoc2 complex as well as HUWE1-mediated allosteric ubiquitination of the Shoc2 scaffold and the RAF-1 kinase. Abrogated ATPase activity leads to augmented ubiquitination of Shoc2/RAF-1 and altered phosphorylation of RAF-1. We found that in fibroblasts from patients with inclusion body myopathy with Paget's disease of bone and frontotemporal dementia (IBMPFD) that harbor germline mutations in VCP, the levels of Shoc2 ubiquitination and ERK1/2 phosphorylation are imbalanced. This study provides a mechanistic basis for the critical role of VCP in the regulation of the ERK1/2 pathway and reveals a previously unrecognized function of the ERK1/2 pathway in the pathogenesis of IBMPFD.

## Monitoring Editor

Carl-Henrik Heldin  
Ludwig Institute for Cancer  
Research

Received: Mar 11, 2019

Revised: Apr 25, 2019

Accepted: May 8, 2019

## INTRODUCTION

Valosin-containing protein (VCP), also known as p97, is an AAA+ ATPase (ATPase associated with a variety of cellular activities) motor protein that regulates a perplexing range of cellular functions (van den Boom and Meyer, 2018). VCP is well known for its role in many pathways of the proteasome system and the endoplasmic reticulum-associated protein degradation system (Lipson *et al.*, 2008). The remarkable diversity of VCP functions is achieved through a multitude of regulatory cofactors, which control substrate specificity and fate, subcellular localization, and the oligomeric state of VCP (Hanzelmann and Schindelin, 2017). In functions such as DNA replication, assembly of nuclear and Golgi membranes, nonproteasomal

degradation through macroautophagy, and the endolysosomal pathway, VCP is involved in remodeling, unfolding, extraction, or "segregation" of a ubiquitinated substrate from stable protein assemblies, membranes, or chromatin (Acs *et al.*, 2011; Meerang *et al.*, 2011; Dantuma and Hoppe, 2012; Chen *et al.*, 2013; van den Boom *et al.*, 2016; Papadopoulos and Meyer, 2017; Ye *et al.*, 2017). The molecular mechanisms underlying the "segregase" activity of the ring-shaped hexameric VCP assembly rely on conformational changes induced by ATP binding and hydrolysis by its two ATPase domains D1 and D2 (Hanzelmann and Schindelin, 2017).

Germline mutations in VCP cause an autosomal dominant and fatal familial disorder called inclusion body myopathy with Paget's disease of bone and frontotemporal dementia (IBMPFD; Watts *et al.*, 2007; Wehl *et al.*, 2009; Piccirillo and Goldberg, 2012). IBMPFD is a multisystemic disease characterized by incomplete penetrance of three main features: disabling muscle weakness, osteolytic bone lesions consistent with Paget's disease, and frontotemporal dementia (Kimonis *et al.*, 2008a,b). At the cellular level, IBMPFD is characterized by impairments in protein degradation and an accumulation of ubiquitinated protein aggregates as well as other cellular defects, while the molecular basis underlying these cellular abnormalities remains elusive. A majority of IBMPFD-associated VCP mutations alter the structural orientation between the VCP N and D1 domains (Tang *et al.*, 2010), thus modifying the recognition by cofactors and/or its ATPase hydrolysis (Fernandez-Saiz and Buchberger, 2010). Being a key mediator of protein

This article was published online ahead of print in MBoC in Press (<http://www.molbiolcell.org/cgi/doi/10.1091/mbc.E19-03-0144>) on May 15, 2019.

<sup>†</sup>These authors contributed equally to this work.

\*Address correspondence to: Emilia Galperin ([emilia.galperin@uky.edu](mailto:emilia.galperin@uky.edu)).

Abbreviations used: ERK1/2, extracellular signal-regulated kinase 1 and 2; IBMPFD, inclusion body myopathy with Paget's disease of bone and frontotemporal dementia; NSLH, Noonan syndrome with loose anagen hair; VCP, valosin-containing protein.

© 2019 Jang, Jang, *et al.* This article is distributed by The American Society for Cell Biology under license from the author(s). Two months after publication it is available to the public under an Attribution-Noncommercial-Share Alike 3.0 Unported Creative Commons License (<http://creativecommons.org/licenses/by-nc-sa/3.0>).

"ASCB®," "The American Society for Cell Biology®," and "Molecular Biology of the Cell®" are registered trademarks of The American Society for Cell Biology.

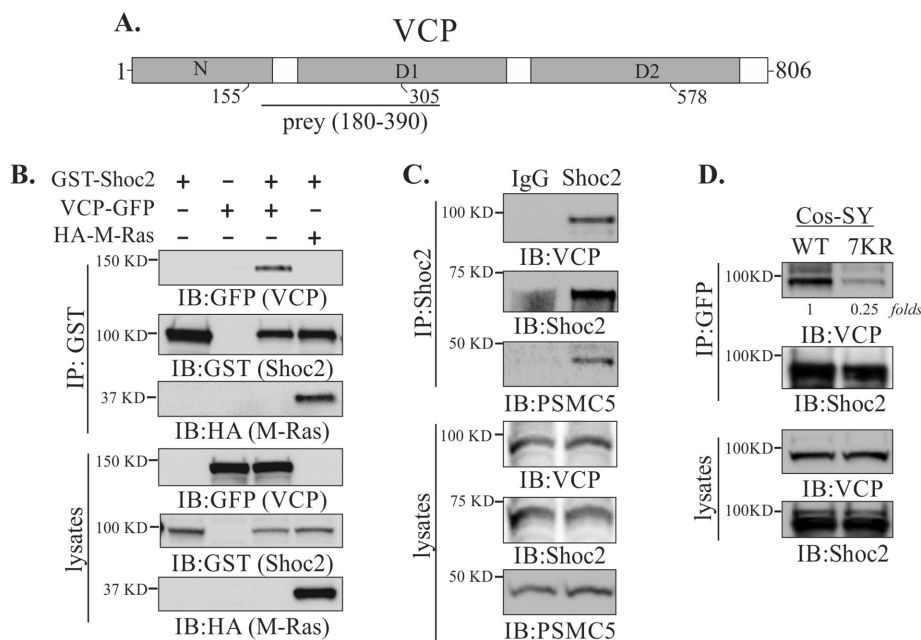


**FIGURE 1:** Shoc2 interacts with VCP. (A) Schematic diagram depicting the domains of VCP protein. The positions of mutants used in this study as well as the prey region of VCP (aa 180–390) obtained in the yeast two-hybrid screening are shown. (B) 293FT cells were cotransfected with VCP-GFP, HA-M-Ras, or GST-Shoc2. VCP-GFP and HA-M-Ras were immunoprecipitated and analyzed by immunoblotting using anti-HA, -GFP, or -GST antibodies. (C) Coimmunoprecipitation of endogenous Shoc2, VCP, and PSMC5. Shoc2, VCP, and PSMC5 antibodies were used to detect VCP and PSMC5 in Shoc2 immunoprecipitates and in total lysates of 293FT cells. (D) GFP-tagged VCP was immunoprecipitated from Cos1 cells depleted of endogenous Shoc2 and stably expressing either YFP-tagged Shoc2 or 7KR mutant Shoc2. VCP and Shoc2 were detected in GFP immunoprecipitates and lysates using anti-VCP and anti-Shoc2 antibodies. The results in each panel are representative of those from three independent experiments.

homeostasis, VCP has emerged as an attractive target for anti-cancer therapy and development of selective ATP-competitive small-molecule compounds like CB-5083 (Anderson *et al.*, 2015; Zhou *et al.*, 2015; Bastola *et al.*, 2016; Vekaria *et al.*, 2016; Gugliotta *et al.*, 2017; Lan *et al.*, 2017).

In this study, we provide evidence that VCP modulates signals of the canonical extracellular signal-regulated kinase (ERK1/2) pathway transduced by the Shoc2 scaffolding module. The scaffolding proteins of the ERK1/2 pathway direct a coordinated effort to govern a myriad of downstream cellular signaling events (Langeberg and Scott, 2015). Scaffolds assemble multicomponent interacting modules to control the specificity, amplitude, and duration of ERK1/2 signals, as well as enhance phosphorylation of specific ERK1/2 substrates (Dhanasekaran *et al.*, 2007; Alexa *et al.*, 2010). Shoc2 is a key modulator of the ERK1/2 pathway, and its silencing or impairments in the assembly of the Shoc2 complex have a prohibitive effect on ERK1/2 activity and disrupt cellular functions (Jang and Galperin, 2016). The detrimental effects of Shoc2 knockout on the embryonic development of mice and zebrafish underscore the central role of Shoc2 in the transmission of ERK1/2 signals (Yi *et al.*, 2010; Jang *et al.*, 2019). Missense mutations in the *shoc2* gene give rise to a developmental disorder with a wide spectrum of physiological and cognitive deficiencies, known as Noonan-like syndrome with loose anagen hair (NSLH; Cordeddu *et al.*, 2009; Hannig *et al.*, 2014).

We and others have shown that Shoc2 assembles an intricate scaffolding complex that includes canonical signaling enzymes (i.e., Ras, RAF-1, and the catalytic subunit of PP1c) as well as the E3 ligase

HUWE1 and the AAA+ ATPase PSMC5, both part of the ubiquitin machinery (Rodríguez-Viciano *et al.*, 2006; Jang *et al.*, 2014, 2015). Together these proteins create an elegant mechanism that accelerates and fine-tunes the amplitude of ERK1/2 signals in a spatially defined manner (Jang and Galperin, 2016). Specifically, within the Shoc2 module, the E3 ligase HUWE1 catalyzes the ubiquitination of Shoc2 and RAF-1 to provide a negative feedback that modulates activity of the ERK1/2 pathway (Jang *et al.*, 2014). Consequently, PSMC5 triggers an essential redistribution of the Shoc2 complexes to late endosomes/multivesicular bodies where HUWE1 is sequestered from the scaffolding complex leading to decreased Shoc2 and RAF-1 ubiquitination (Jang *et al.*, 2015).

Here, we show that VCP is critical for the coordinated feedback mechanisms modulating the ERK1/2 signals via the Shoc2–Ras–RAF-1 complex. Importantly, our findings demonstrate that alterations in Shoc2 ubiquitination and ERK1/2 phosphorylation are also important elements of IBMPFD pathology.

## RESULTS AND DISCUSSION

### VCP is a novel partner in the Shoc2 scaffold module

To elucidate the molecular mechanisms controlling ERK1/2 signals, we performed the yeast two-hybrid screen of a human adult/fetal heart library (Jang *et al.*, 2014, 2015). The yeast two-hybrid screen using full-length Shoc2 as a bait detected 29 cDNA prey fragments all within amino acids 180–390 of the 97 kDa AAA+ ATPase VCP. All of the isolates extended over the carboxy terminus of the N domain and part of the D1 domain connected by an interdomain linker (N–D1) of VCP (Figure 1A).

To validate the Shoc2 and VCP interaction, we coexpressed glutathione *S*-transferase (GST)–fused Shoc2 (GST-Shoc2) and GFP-tagged VCP (VCP-GFP) in 293FT cells. VCP was detected in the GST immunoprecipitate, indicating the association of VCP and Shoc2 (Figure 1B). Coimmunoprecipitation of endogenous Shoc2 with HA-M-Ras and VCP, PSMC5 from 293FT cells further validated that these proteins form a quaternary complex (Figure 1, B and C).

VCP is known to be associated with the recognition of ubiquitinated substrates (Dantuma and Hoppe, 2012). Thus, to examine whether VCP recognizes modified Shoc2, we utilized the 7KR (seven lysines mutated to arginines) mutant of Shoc2 for which ubiquitination levels are 70–80% lower than those of wild-type (WT) Shoc2 (Jang *et al.*, 2014). The interaction of VCP and Shoc2 was assessed by immunoprecipitation using Cos1 cells stably expressing either WT or the 7KR mutant of Shoc2-YFP and depleted of endogenous Shoc2 (Jang *et al.*, 2014). The amount of VCP in the Shoc2 (7KR) mutant immunoprecipitate was decreased dramatically, indicating that VCP is associated with ubiquitinated Shoc2 (Figure 1D). Additionally, we mapped the VCP-recognition region to the leucine-rich repeats 12–14 (aa 347–417) of Shoc2 (Supplemental Figure 1). Interestingly, the leucine-rich repeats 12–14 also constitute the HUWE1 binding domain (Supplemental Figure 1E; Jang *et al.*, 2014).

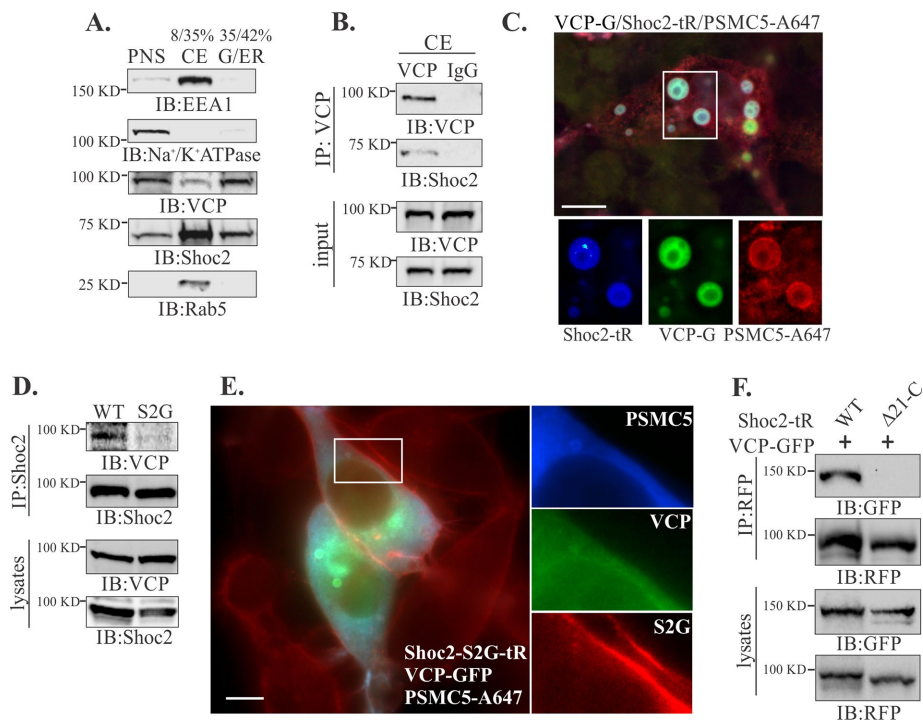


**FIGURE 2:** VCP is in complex with Shoc2 on endosomes. (A) Post nuclear supernatants (PNSs) from Cos1 cells were layered on 8–42% sucrose gradients and subjected to ultracentrifugation. The indicated proteins were identified by immunoblotting (IB) using specific antibodies in crude endosome (CE) or Golgi and endoplasmic reticulum (G/ER) fractions. (B) VCP was immunoprecipitated from the crude endosomal fraction and analyzed by using specific anti-VCP and Shoc2 antibodies. (C) Cos-SR cells depleted of endogenous Shoc2 and stably expressing Shoc2-tRFP were transfected with VCP-GFP and GST-PSMC5, permeabilized with 0.05% saponin and then fixed, immunostained for GST, and followed by immunofluorescence microscopy. Insets show high-magnification images of the region indicated by white rectangles. Scale bars: 10  $\mu$ m. (D) Shoc2 was immunoprecipitated from Cos-SR cells depleted of endogenous Shoc2 and stably expressing WT or S<sup>2</sup>G mutant Shoc2-tRFP. The immunoprecipitates were analyzed with anti-VCP and -Shoc2 antibodies. (E) Cos1 cells stably expressing the Shoc2-S<sup>2</sup>G mutant (Shoc2-S<sup>2</sup>G-tR) were transfected with GST-PSMC5 and VCP-GFP. GST-PSMC5 was immunostained with anti-GST antibody. Cells were fixed and followed by immunofluorescence microscopy. Insets show high-magnification images of the regions of the cell indicated by white rectangles. Scale bars: 10  $\mu$ m. (F) Cos1 cells depleted of endogenous Shoc2 and stably expressing either full-length Shoc2-tRFP (WT) or the mutant of Shoc2 ( $\Delta$ 21-C) were transfected with VCP-GFP. Shoc2 was immunoprecipitated using anti-RFP antibodies. The immunoprecipitates were analyzed by immunoblotting using anti-RFP and -GFP antibodies. The results in each panel are representative of those from three independent experiments.

Together, these results demonstrate that VCP is a previously unrecognized interacting partner in the Shoc2–Ras–RAF-1 signaling scaffold complex.

Shoc2 multiprotein complexes are targeted to endosomes upon activation of the ERK1/2 pathway (Galperin *et al.*, 2012; Jang *et al.*, 2015). To delineate how VCP affects cellular distribution of the Shoc2 module, the localization of Shoc2–VCP complexes was analyzed using complementary methods of subcellular fractionation and fluorescence microscopy (Figure 2). A crude endosomal fraction (late and early endosomes; CE) from Cos1 cells was enriched by using discontinuous sucrose density gradient centrifugation where CE was at the 8/35% interface of the gradient (de Araujo *et al.*, 2008). The distribution of the key markers of early endosomes (EEA1/Rab5) and plasma membrane (Na<sup>+</sup>/K<sup>+</sup>-ATPase) indicates that CE as well as Golgi and endoplasmic reticulum (G/ER) fractions were free of any significant amount of plasma membranes (Figure 2A). VCP readily precipitates Shoc2 from the recovered CE protein interface, indicat-

ing that VCP redistributes to the endosomes together with Shoc2 (Figure 2B). The total amount of homogenate was comparable to the amount of total lysate used in the immunoprecipitation experiments in Figure 1.

Furthermore, we examined the localization of endogenous Shoc2 and expressing Shoc2-tRFP together with the oligomeric PSMC5 (GST-PSMC5) that triggers Shoc2 recruitment to late endosomes/multivesicular bodies (LE/MVBs; Jang *et al.*, 2015). Immunofluorescence microscopy revealed that a majority of Shoc2-tRFP and GST-PSMC5 positive vesicles also contained VCP-GFP (Figure 2C). Many of the Shoc2-tRFP/GST-PSMC5/VCP-GFP positive vesicles often had multimembrane intraluminal branches characteristic of large multivesicular bodies and in some instances reached 4–5  $\mu$ m in size, likely as a result of membrane fusion induced by the accumulation of Shoc2-PSMC5 complexes. These vesicular structures were previously characterized as the late endosomal compartments (Jang *et al.*, 2015).

The NSLH causative S<sup>2</sup>G mutant of Shoc2 that is mislocalized to the plasma membrane due to aberrant N-terminal myristoylation was used to explore the impact of subcellular localization on the Shoc2–VCP complex (Cordeddu *et al.*, 2009; Galperin *et al.*, 2012). Surprisingly, VCP was almost undetectable in the Shoc2 immunoprecipitates obtained from the cells stably depleted of endogenous Shoc2 and expressing the S<sup>2</sup>G Shoc2-tRFP mutant (Figure 2D), indicating that Shoc2–VCP complexes are formed in a spatially defined manner, likely on endosomes. Immunofluorescence microscopy of cells expressing Shoc2 (S<sup>2</sup>G)-tRFP, VCP-GFP, and GST-PSMC5 confirmed findings in Figure 2D by showing no colocalization of VCP with the Shoc2 (S<sup>2</sup>G) mutant (Figure 2E). To further shed light on the

requirements for the correct spatial distribution of the Shoc2–VCP complex, we utilized the Shoc2  $\Delta$ 21-C mutant lacking its PSMC5 binding domain (Jang *et al.*, 2015). This mutant of Shoc2 is excessively ubiquitinated and unable to translocate to the endosomal compartment (Jang *et al.*, 2015). The  $\Delta$ 21-C mutant of Shoc2 was also impaired in its ability to associate with VCP (Figure 2F), indicating that VCP recognizes ubiquitinated Shoc2 only when Shoc2 is recruited to endosomes. Therefore, we hypothesize that VCP is essential for remodeling the Shoc2 complex on endosomes and its function is complementary to the function of PSMC5 in the complex.

#### VCP modulates ubiquitination of Shoc2 on endosomes

VCP uses ATP as an energy source to remodel (unfold/segregate) ubiquitinated substrates from a variety of macrocomplexes and cellular locations, facilitating their degradation and/or recycling (Ye *et al.*, 2017). To explore a possible role of VCP in the remodeling of

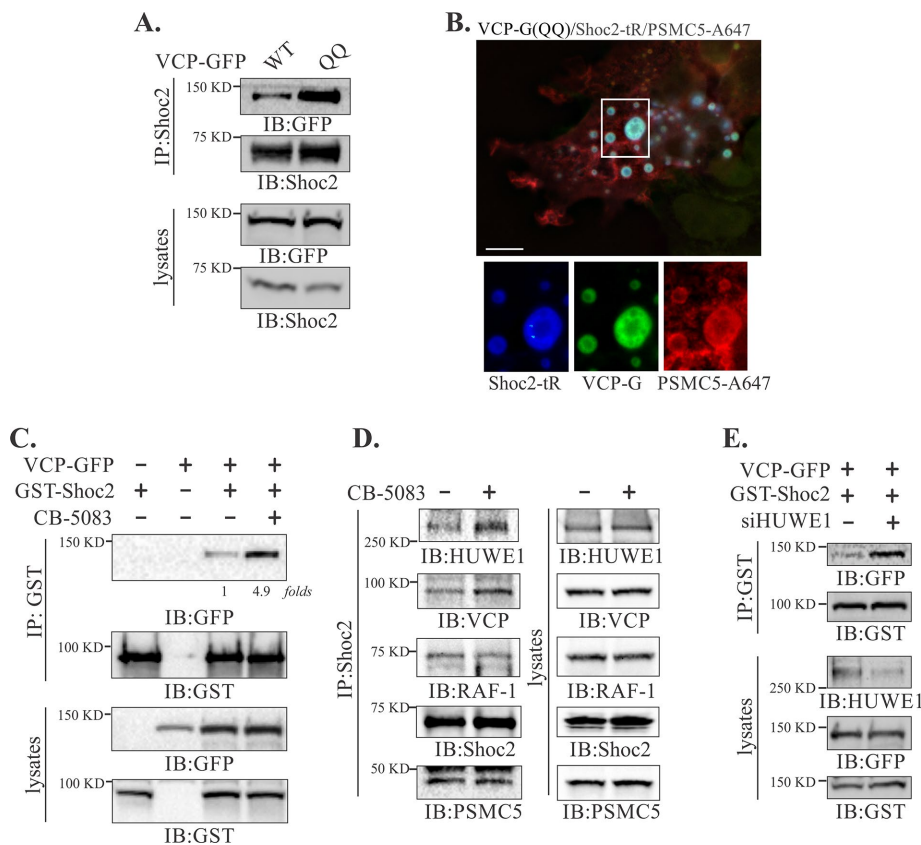


**FIGURE 3:** ATPase activity of VCP is necessary to modulate the interaction of Shoc2 with HUWE1. (A) Endogenous Shoc2 was immunoprecipitated from 293FT cells transfected with wild-type (WT) or catalytically inactive (QQ) mutant of VCP-GFP using anti-Shoc2 antibody. The immunoprecipitates were analyzed by immunoblotting using anti-GFP and -Shoc2 antibodies. (B) Cos-SR cells (depleted of endogenous Shoc2 and stably expressing Shoc2-tRFP) expressing the QQ mutant of VCP-GFP and GST-PSMC5 were fixed, immunostained for GST, followed by immunofluorescence microscopy. Insets show high-magnification images of the region indicated by white rectangles. Scale bars: 10  $\mu$ m. (C) 293FT cells were cotransfected with VCP-GFP and GST-Shoc2. Cells were then treated with the vehicle (dimethyl sulfoxide [DMSO]) or 5  $\mu$ M of CB-5083 for 4 h. GST-Shoc2 immunoprecipitates were analyzed using anti-GST and -GFP antibody antibodies. (D) Endogenous Shoc2 was immunoprecipitated from Cos1 cells treated with vehicle (DMSO) or 5  $\mu$ M of CB-5083 for 4 h. The immunoprecipitates were analyzed by immunoblotting with using anti-VCP, -HUWE1, RAF-1, Shoc2, and -PSMC5 antibodies. (E) GST-Shoc2 was immunoprecipitated from 293FT cells cotransfected with VCP-GFP and GST-Shoc2 and depleted in HUWE1. The immunoprecipitates were analyzed using anti-GFP and -GST antibodies. The results in each panel are representative of those from three independent experiments.

Shoc2 complexes, we expressed the ATPase activity deficient QQ mutant of VCP (E<sup>305</sup>Q, E<sup>578</sup>Q) or treated cells with the VCP ATP-competitive chemical inhibitor CB-5083 (Anderson *et al.*, 2015). Of note, CB-5083 has no effect on the levels of the proteins in the Shoc2 complex (Supplemental Figure 2A) and does not affect the ATPase activity of PSMC5 (Anderson *et al.*, 2015). Under the experimental conditions with overexpression of the VCP QQ mutant, accumulation of the ATP-activity deficient VCP in the Shoc2 scaffolding complex was detected (Figure 3A). Importantly, the ATPase activity deficient QQ mutant was easily detectable on Shoc2-PSMC5 positive endosomes (Figure 3B), suggesting that enzymatic activity of VCP is not required for Shoc2-VCP recognition and the subcellular distribution of the Shoc2 complex. These conclusions were supported further by the findings that, although deficient in VCP association, the Shoc2 (7KR) mutant can be recruited to endosomes as effectively as its WT counterpart (Supplemental Figure 3, A and B).

Similarly, treatment with CB-5083 that selectively competes for ATP binding at the D2 ATPase domain responsible for the majority of the VCP's ATPase activity resulted in increased amounts of VCP in GST-Shoc2 immunoprecipitates (Figure 3C). These data show that loss of ATP activity results in the accumulation of VCP in the Shoc2 complex. Furthermore, we found that in cells treated with CB-5083, the E3 ligase HUWE1 also accumulates in the Shoc2 complex (Figure 3D and Supplemental Figure 2B). Interestingly, inhibited VCP activity had no effect on the presence of RAF-1 and PSMC5 in the complex (Figure 3D). Given the overlap in the Shoc2 recognition domains of VCP and HUWE1 (Supplemental Figure 1, D and E), we investigated whether VCP and HUWE1 cooperate functionally in the Shoc2 complex. Indeed, in cells depleted of HUWE1, increased amounts of VCP immunoprecipitated with Shoc2 (Figure 3E), suggesting that HUWE1 is likely to accelerate the mechano-activity of VCP and facilitate its disassembly. Similar modes of action were shown for other AAA+ ATPases (Hanson and Whiteheart, 2005). However, future studies are needed to provide additional details into the underlying mechanisms. These data also suggest that the ATPase activity of VCP is a contributing factor into the assembly/disassembly or "segregation" of the proteins from the Shoc2 signaling module.

We have previously reported that the E3 ligase HUWE1 mediates ubiquitination of Shoc2, RAF-1, and the kinase activity of RAF-1 (Jang *et al.*, 2014). Thus, the data in Figure 3D strongly indicate that the ATPase activity of VCP may regulate the levels of Shoc2 and RAF-1 ubiquitination catalyzed by HUWE1. To test this notion, we treated Cos1 cells with CB-5083 and examined the ubiquitination of Shoc2 and RAF-1 under denaturing conditions. Cells treated with CB-5083 or cells expressing the VCP QQ mutant had markedly increased levels of ubiquitinated Shoc2 and RAF-1 (Figure 4, A and B, and Supplemental Figure 4A). HUWE1-mediated Shoc2 ubiquitination is induced by activation of epidermal growth factor receptor (EGFR) and its time course closely follows the ERK1/2 phosphorylation curve (Figure 4C, lanes 1–4, and our previous studies, Jang *et al.*, 2014, 2015). Conversely, in the cells treated with CB-5083, sustained Shoc2 ubiquitination irrespective of the ERK1/2 phosphorylation status was detected (Figure 4C, lanes 5–8). In agreement with data in Figure 4C, CB-5083 treatment led to the accumulation of VCP and HUWE1 in Shoc2 immunoprecipitate from the CE (Figure 4D). The levels of ubiquitinated Shoc2 precipitated from the endosomal fraction of cells treated with CB-5083 were also significantly higher than in control cells (Figure 4E), while the overall ubiquitination of the proteins in the CE fraction was comparable. Taken together, the above results show that VCP functions as a modulator of Shoc2 and RAF-1 ubiquitination.

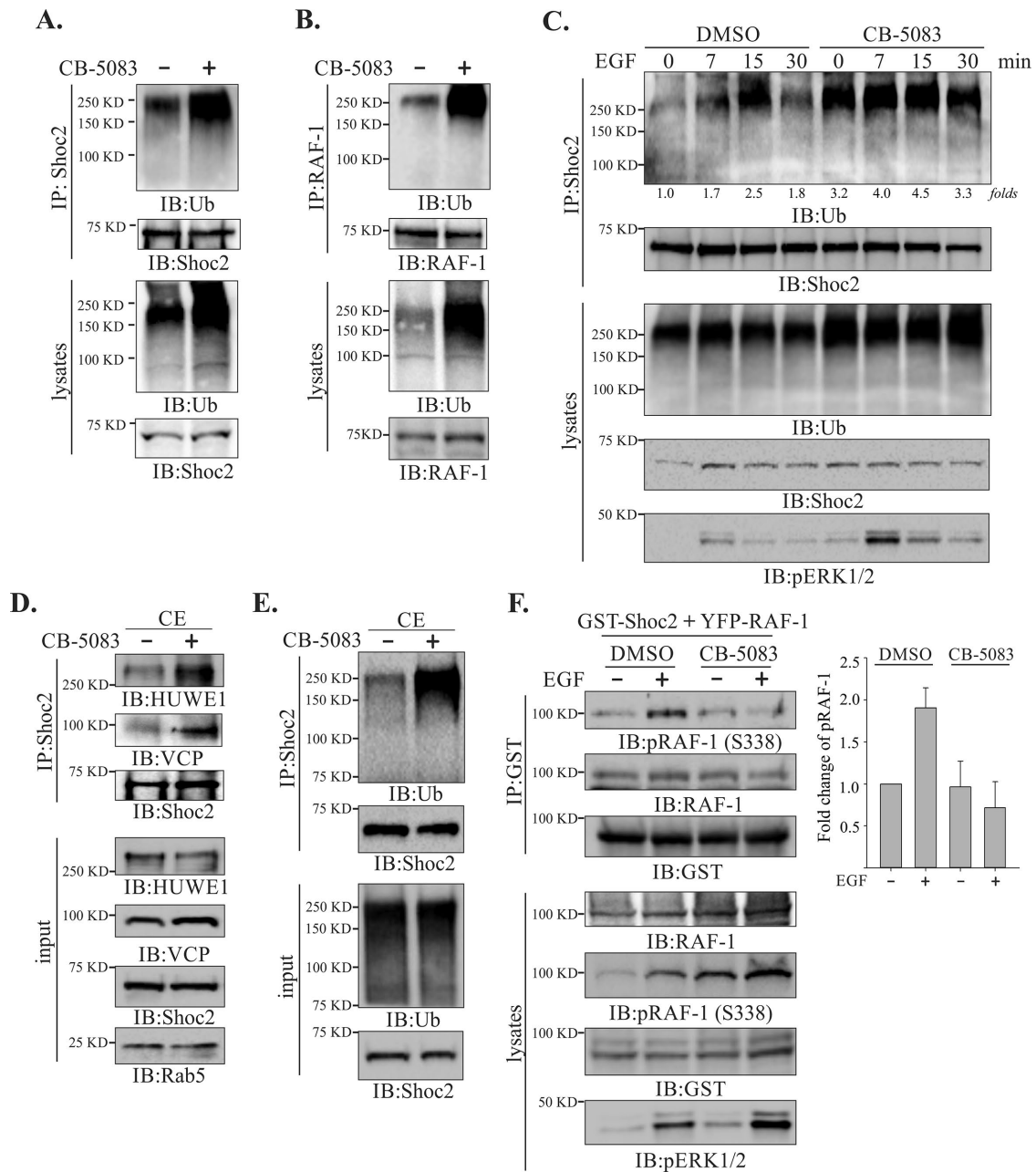


**FIGURE 4:** VCP controls levels of ubiquitination of Shoc2 and affects RAF-1/ERK1/2 activation. (A, B) Endogenous Shoc2 (A) or RAF-1 (B) was immunoprecipitated from denatured cell lysates of Cos1 cells treated with 5  $\mu$ M of CB-5083 for 4 h. Shoc2 and RAF-1 ubiquitination was detected by immunoblotting using anti-ubiquitin (Ub) antibody. (C) Cos1 cells were serum-starved for 16 h, treated with 5  $\mu$ M of CB-5083 for 4 h, and then stimulated with EGF (0.2 ng/ml) for 7, 15, and 30 min. Endogenous Shoc2 was precipitated from denatured cell lysates using anti-Shoc2 antibodies and its ubiquitination was detected with anti-ubiquitin (Ub) antibody. Immunoblots were analyzed with anti-Shoc2, -Ub, and -pERK1/2 antibodies. (D) Crude endosomal (CE) subcellular fractions were prepared from Cos1 cells treated with vehicle (DMSO) or 5  $\mu$ M of CB-5083 for 4 h. Endosomal Shoc2 was immunoprecipitated and analyzed using the indicated antibodies. Rab5 was used as a loading control. (E) Shoc2 was precipitated from denatured endosomal fractions prepared in D using anti-Shoc2 antibodies. Shoc2 ubiquitination was detected with anti-Ub antibody. (F) Cos1 cells were transfected with GST-Shoc2 and YFP-RAF-1. At 48 h posttransfection, cells were serum-starved for 16 h and treated with vehicle (DMSO) or 5  $\mu$ M of CB-5083 for 4 h and then stimulated with EGF (0.2 ng/ml) for 7 min. Shoc2 was immunoprecipitated using anti-GST antibody. Immunoblots were analyzed with anti-p-RAF-1 (S338), -RAF-1, -GST, and -pERK1/2 antibodies. Blots from the multiple experiments were analyzed. Bars represent the mean  $\pm$  SE ( $n = 3$ ) for pRAF-1 normalized to the value for GAPDH in arbitrary units ( $p < 0.01$ , by Student's  $t$  test). The results in each panel are representative of those from three independent experiments.

Surprisingly, these experiments also revealed that the amplitude of phospho-ERK1/2 in the cells treated with CB-5083 was significantly higher than in control cells. These findings are in contrast with the previously understood role of Shoc2 ubiquitination as being a negative-feedback mechanism to fine-tune the ERK1/2 phosphorylation (Jang *et al.*, 2014). Thus, activation of RAF-1 kinase coupled with the Shoc2 scaffold was examined. Phosphorylation of RAF-1 at Ser338 was compared in Shoc2 immunoprecipitates from cells treated with CB-5083 to immunoprecipitates from control cells. In control cells, phosphorylation of the Shoc2-bound RAF-1 increased twofold in response to the EGFR stimulation (Figure 4F). However, in cells treated with CB-5083 no changes in RAF-1 phosphorylation were observed. Yet, total levels of phospho-ERK1/2 were higher in the cells treated with the inhibitor. Given the multitude of VCP-controlled cellular functions, it is possible that loss of the VCP-ATPase activity deregulates negative-feedback loops targeting other com-

ponents of the ERK1/2 network or rather induces activation of ERK1/2 via an alternative signaling loop or by kinases other than RAF-1. Teasing apart precise loops that activate ERK1/2 upon CB-5083 inhibition will require further investigation. Nevertheless, we conclude that in the Shoc2 scaffolding module, VCP is likely to regulate the HUWE1-mediated Shoc2 ubiquitination by sequestering the E3 ligase HUWE1 from the complex. Thus, our data suggest that VCP is recruited to the endosomal compartment together with Shoc2 where VCP's ATPase mechanoenzyme activity is exerted to remodel the Shoc2 scaffolding complex, regulating the Shoc2-routed RAF-1/ERK1/2 signals.

### The Shoc2/ERK1/2 nexus in IBMPFD pathogenesis

The IBMPFD-causing mutations have significant effects on VCP binding to cofactors as well as its enzymatic activity (Mountassif *et al.*, 2015). Hence, we tested whether the most-common disease-

related mutation of VCP (Arg<sup>155</sup>His, R<sup>155</sup>H) affects ubiquitination of Shoc2. To address this question, we expressed the R<sup>155</sup>H mutant of VCP or its WT counterpart in Cos1 cells and examined the ubiquitination of Shoc2. Expression of the VCP R<sup>155</sup>H mutant led to an increased Shoc2 ubiquitination, whereas expression of its WT counterpart had an opposite effect on ubiquitination of Shoc2 (Figure 5A). Next, we analyzed the VCP-Shoc2 interaction under the pathologically relevant conditions using cultured primary fibroblasts from three IBMPFD patients, all expressing VCP proteins altered in the mutational hotspot, R<sup>155</sup>H. Fibroblasts from a healthy relative were used as a baseline. Significantly higher ubiquitination of Shoc2 was detected when it was immunoprecipitated from IBMPFD fibroblasts (Figure 5B). Accordingly, we found increased levels of RAF-1 ubiquitination in Cos1 cells expressing the VCP R<sup>155</sup>H mutant and in IBMPFD patient fibroblasts (Supplemental Figure 4, B and C). Importantly, the steady-state levels of phospho-ERK1/2 were significantly higher in IBMPFD fibroblasts compared with normal fibroblasts (Figure 5B), which was strikingly similar to what we observed in cells treated with the VCP inhibitor CB-5083 (Figure 4, C and F). Thus, our data further emphasize that aberrations in the function of VCP are likely to trigger compensatory network responses that are no longer under the tight fine-tuning of the Shoc2 scaffold. Together, our results show that VCP is required to balance levels of ERK1/2 activation (Figure 5C).

### Conclusions

Studies presented here provide new insights into the mechanism modulating ubiquitination of Shoc2, RAF-1, and transmission of signals through the Shoc2 scaffolding complex. These studies are the first to identify the AAA+ ATPase VCP as a critical element in the ERK1/2 pathway. We present

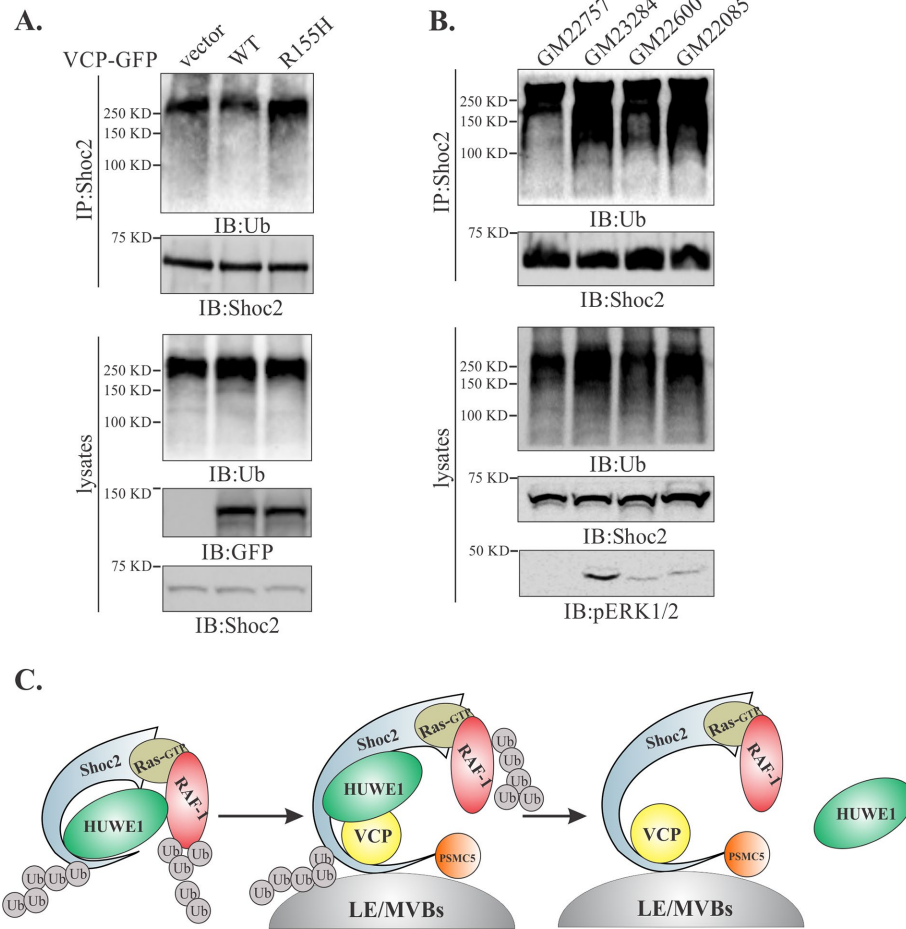


**FIGURE 5:** Ubiquitination of Shoc2 and RAF-1 is altered in fibroblasts from IBMPFD patients. (A) Endogenous Shoc2 was precipitated from the denatured cell lysates of Cos1 cells expressing WT or R<sup>155</sup>H mutant of VCP-GFP. Shoc2 ubiquitination was detected with anti-Ub antibody. (B) Endogenous Shoc2 was immunoprecipitated from the denatured lysates of primary fibroblast using anti-Shoc2 antibodies. GM23284, GM22600, and GM22085—fibroblasts harboring VCP R<sup>155</sup>H mutation; GM22757—normal relative control. Shoc2 ubiquitination was detected with anti-Ub antibody. pERK1/2 was analyzed using specific pERK1/2 (p42/44) antibodies. The results in each panel are representative of those from three independent experiments. (C) Working model depicting what is currently understood for the mechanisms modulating the Shoc2-mediated ERK1/2 signals. Activation of the ERK1/2 pathway is followed by HUWE1-mediated ubiquitination of Shoc2 and RAF-1 causing the adjustments in the amplitude of ERK1/2 signaling. Thereafter, PSMC5 facilitates the recruitment of the Shoc2 complex to endosomes where VCP recognizes ubiquitinated Shoc2 and HUWE1 and sequesters or “segregates” HUWE1 from the Shoc2 complex, possibly aiding in the “reactivation” of the Shoc2 signaling module.

compelling evidence that VCP is an integral partner in the Shoc2 signaling module (Figures 1 and 2) showing that VCP is associated with ubiquitinated Shoc2 (Figures 3 and 4). Given VCP association with a set of adaptors or cofactors that assist in the recognition of ubiquitinated proteins, it is unlikely that VCP recognizes Shoc2 without the assistance of a cofactor, but its identity is yet to be determined. Our findings of VCP and HUWE1 competitive binding to the scaffold delivered a critical clue to the model in Figure 5C and were consistent with the observations that perturbations in the ATPase activity of VCP lead to the increased presence of HUWE1 in the Shoc2 complex and altered levels and dynamics of Shoc2 ubiquitination (Figure 4).

In this model, VCP exerts its mechanoactivity to “sequester” the E3 ligase HUWE1 from the Shoc2 scaffolding complex in order to modulate levels of ubiquitin conjugated to Shoc2, which is in agreement with the core biochemical activity of VCP to segregate components from multimolecular structures (Meyer *et al.*, 2012; Blythe *et al.*, 2017). However, it is not clear which one of the proteins in the Shoc2 complex is an immediate VCP substrate that undergoes unfolding. If Shoc2 is a substrate, then it is plausible that, in addition to the sequestration of HUWE1 from the complex, an unfolding of Shoc2 may also result in the loss of RAF-1 or in an orientation unfavorable for signal transmission. This scenario, however, requires further studies using methodologies that can reconstitute remodeling events in the Shoc2 scaffolding complex *in vitro*.

The processing of VCP substrates is contingent on the binding of K48- and K11/K48-conjugated ubiquitin chains by VCP and/or its adaptors (Wojcik *et al.*, 2004; Jentsch and Rumpf, 2007; Meerang *et al.*, 2011). In the recent study by Heidelberg *et al.* (2018), VCP was linked to the ubiquitination assembled by the E3 ligase HUWE1 via K6-ubiquitin linkages and c-myc activation. Thus, it will be important to determine the specific Shoc2-ubiquitin links that are recognized by VCP.

Importantly, results presented here are also in agreement with earlier observations demonstrating that the ubiquitination of Shoc2 is controlled in a spatially restricted manner (Jang *et al.*, 2014, 2015). Much like the E3 ligase HUWE1 and AAA+ ATPase PSMC5, VCP was found in the complex with WT Shoc2 when targeted to the endosomal membranes. In contrast, VCP failed to recognize the aberrantly targeted to the plasma membrane Shoc2 (S<sup>2</sup>G) mutant or the mutant that fails to interact with PSMC5 (Figure 2). An increased ubiquitination of the endosome-localized Shoc2 in cells treated with CB-5083 further emphasizes the role endosomes play in supporting the specific microenvironmental requirement for the regulation of signaling.

One unexpected observation was that in the cells treated with CB-5083 we consistently detected increased phospho-ERK1/2 response (Figure 4). This prompted us to hypothesize that an abnormal function of VCP not only affects regulatory mechanisms within the Shoc2 complex but also misbalances a tightly controlled ERK1/2 signaling network. CB-5083 is currently explored as an approach to target the proteasomal response in solid and liquid malignancies (Anderson *et al.*, 2015; Le Moigne *et al.*, 2017; Gareau *et al.*, 2018). Our findings that VCP inhibition increases ERK1/2 phosphorylation and likely affects downstream transcription needs to be taken into account when clinical effects of VCP inhibitors are evaluated for anti-tumor activity.

Another key finding of this study is that IBMPFD-causing mutations in VCP perturb ERK1/2 phosphorylation is the evidence that elevated ERK1/2 activity contributes to the IBMPFD pathogenesis. These data provide a molecular rationale for exploring strategies to manage ERK1/2 activity in IBMPFD patients. However, given the contextual roles of ERK1/2 activation in cell survival and death, pharmacological modulation of this signaling pathway is likely to

demand careful optimization. Importantly, this study is the first to suggest a possible involvement of aberrant ERK1/2 signaling in the pathogenesis of IBMPFD. Future studies will aid in understanding the full extent of the mechanisms causing the disease.

Collectively, our findings of VCP as an essential component in Shoc2-mediated signaling, establish a novel role for this ATPase in regulating the canonical ERK1/2 signaling pathway. This study not only provides new insights into the signaling mechanisms but also underscores how vital it is to understand the molecular and cellular basis of diseases for dissecting disease pathogenesis and designing effective management strategies. Further study is needed to clarify the pathophysiological significance of the interaction between Shoc2 and VCP in neurodegenerative disorders.

## MATERIALS AND METHODS

### Antibodies and other reagents

EGF was obtained from BD Biosciences. Antibodies against the following proteins were used: RAF-1, GST, GFP, HA, phosphorylated ERK1/2 (pERK1/2), and glyceraldehyde 3-phosphate dehydrogenase (GAPDH) (Santa Cruz Biotechnology, Dallas, TX); Shoc2 (Proteintech, Rosemont, IL); EEA1 and phosphorylated RAF-1 (pRAF-1; Cell Signaling, Danvers, MA); Rab5 (BD Bioscience, San Jose, CA); RFP and Na<sup>+</sup>/K<sup>+</sup>-ATPase (Thermo Scientific, Waltham, MA); VCP (BioLegend, San Diego, CA); HUWE1 (Bethyl, Montgomery, TX); and ubiquitin (Covance, Princeton, NJ); CB-5083 was kindly provided by Cleave Biosciences (Burlingame, CA).

### Yeast two-hybrid screening assays

Full-length human Shoc2 was cloned into the *lexA* vector pB27 as an N-LexA-Shoc2-C fusion and screened against a human embryo ventricle and heart prey cDNA library. Yeast two-hybrid screens were performed by Hybrigenics SA (Cambridge, MA).

### Cell culture, constructs, and transfections

293FT cells (Invitrogen, Carlsbad, CA), Cos1 (American Type Culture Collection, Manassas, VA), and stable cell lines (SR, SY, S<sup>2</sup>G, Δ21-C; derivative of Cos1 cells) were grown in DMEM (Sigma, St. Louis, MO) containing 10% fetal bovine serum. Shoc2-tRFP, Shoc2-YFP, and Shoc2-7KR-YFP were described previously (Jang *et al.*, 2014). Normal fibroblasts (GM22757) and IBMPFD patient fibroblasts (GM23284, GM22600, GM22085) were obtained from Coriell Institute (Camden, NJ) and were maintained in FibroLife S2 cell culture medium containing FibroLife S2 LifeFactors (Lifeline Cell Technology, Frederick, MD). VCP-GFP constructs (WT, R<sup>155</sup>H, E<sup>305</sup>Q/E<sup>578</sup>Q) were purchased from Addgene (plasmid #23971, #23972, #23974; Watertown, MA). The transfection of DNA constructs was performed using PEI (Neo Transduction Laboratories, Lexington, KY) reagents.

### Small interfering RNA transfections

To silence protein expression, small interfering RNA (siRNA) transfections were performed at 24–36 h intervals according to the manufacturer's recommendations, using DharmaFECT reagent 2 (Thermo Fisher Scientific/Dharmacon, Waltham, MA). The siRNA sequence used to target the HUWE1 and Shoc2 transcripts was described previously (Jang *et al.*, 2014).

### Immunofluorescence staining and analysis

Cells were grown on glass-bottom dishes and washed with Ca<sup>2+</sup>, Mg<sup>2+</sup>-free phosphate buffered saline (CMF-PBS). For immunostaining with anti-GST antibodies, cells were permeabilized with 0.05% saponin to reduce cytosol before cell fixation with freshly prepared 4% paraformaldehyde (Electron Microscopy Sciences, Hatfield, PA)

for 10 min at room temperature. Immunostaining was performed according to manufacturer's recommendations for the antibodies used. All images were acquired using a Marianas imaging system consisting of a Zeiss inverted microscope equipped with a cooled CCD CoolSnap HQ (Roper Technologies, Lakewood Ranch, FL), dual filter wheels, and a Xenon 175 W light source, all controlled by SlideBook software (Intelligent Imaging Innovations, Denver, CO). Image analysis was performed using the SlideBook 6 software. Colocalization analysis was performed using the colocalization statistical module in SlideBook 6 software.

### Sucrose gradient subcellular fractionation

Sucrose gradient subcellular fractionation was performed as described previously (de Araujo *et al.*, 2008; Jang *et al.*, 2015). Briefly, Cos1 cells were grown on 15-cm dishes and then washed and scraped with a rubber policeman in cold PBS. The cells were then pelleted, resuspended in homogenization buffer (250 mM sucrose, 3 mM imidazole, pH 7.4, protease and phosphatase inhibitors, and 0.03 mM cycloheximide) and homogenized using a 22G needle. Homogenization was carried out until ~90% of cells were broken without major breakage of the nucleus, as carefully monitored by microscopy. The samples were centrifuged for 10 min at 2000 g at 4°C and the resulting supernatant was designated as the post nuclear supernatant (PNS). The PNSs were adjusted to 40.6% sucrose concentration using 62% sucrose and then overlaid with 1.5 volumes of 35% sucrose and the rest of the tube was filled with 8.6% sucrose. Sucrose gradients were centrifuged for 6 h at 100,000 × g at 4°C, and the crude endosomal fraction and Golgi and ER membrane fraction were collected.

### Immunoprecipitation and Western blot analysis

Cells were placed on ice and washed with Ca<sup>2+</sup>, Mg<sup>2+</sup>-free PBS, and the proteins were solubilized in 50 mM Tris (pH 7.5) containing 150 mM NaCl, 1% Triton X-100, 1 mM Na<sub>3</sub>VO<sub>4</sub>, 10 mM NaF, 0.5 mM phenylmethylsulfonyl fluoride (Sigma, St. Louis, MO), 10 μg/ml leupeptin, and 10 μg/ml aprotinin (Roche, Basel, Switzerland) for 15 min at 4°C. Lysates were then centrifuged at 14,000 rpm for 15 min to remove insoluble material. Lysates were incubated with appropriate antibodies for 2 h, and the immunocomplexes were precipitated using protein A- or G-sepharose (GE Healthcare Life Sciences, Chicago, IL). In the experiments when crude endosomal fractions were used, Triton X-100 concentration was adjusted to 0.25%. Immunoprecipitates and aliquots of cell lysates were denatured in the sample buffer at 95°C, resolved by electrophoresis, and probed by Western blotting with various antibodies, followed by chemiluminescence detection.

Western blotting was done as described previously (Jeoung *et al.*, 2013). Proteins transferred from SDS-polyacrylamide gels to nitrocellulose membranes were visualized using a ChemiDoc analysis system (Bio-Rad, Hercules, CA). Several exposures were analyzed to determine the linear range of the chemiluminescence signals. Quantification was performed using the densitometry analysis mode of Image Lab software (Bio-Rad, Hercules, CA).

### Denaturing immunoprecipitation for in vivo ubiquitination assay

To study protein ubiquitination, denaturing immunoprecipitations were performed as described previously (Jang *et al.*, 2015). Briefly, cells were lysed in denaturing buffer (50 mM Tris, pH 7.5, 150 mM NaCl, 1% Triton X-100, 1% SDS, 1 mM Na<sub>3</sub>VO<sub>4</sub>, 10 mM NaF, 5 mM NEM, 10 μM MG132) and boiled for 10 min. Lysates were diluted 1:10 with the same buffer without SDS and incubated with the

appropriate antibody overnight with rotation at 4°C. Protein G-agarose was added, and the agarose beads were washed four times in lysis buffer (without SDS). Proteins were eluted at 95°C in SDS loading buffer, separated by SDS-PAGE, and transferred to nitrocellulose membrane.

### Statistical analyses

Results are expressed as means ± SE. The statistical significance of the differences between groups was determined using either Student's *t* test or one-way analysis of variance (followed by the Tukey's test). *p* < 0.05 was considered statistically significant. All statistical analyses were carried out using SigmaStat 13.0 (Systat Software, Chicago, IL).

### ACKNOWLEDGMENTS

We thank Tianyan Gao, Louis Hersh, Charles Waechter, and Craig Vander Kooi for providing reagents and critical reading of the manuscript. The UK Flow Cytometry and Cell Sorting core facility is supported in part by the UK Office of the Vice President for Research, the Markey Cancer Center, and an NCI Center Core Support Grant (Grant no. P30 CA177558). This project was supported by grants from the National Cancer Institute (Grant no. R00CA126161 to E.G.), the National Institute of General Medical Sciences (Grant no. GM113087 to E.G.), the American Cancer Society (Grant no. RSG-14-172-01-CSM to E.G.), and the American Heart Association (Grant no. 15PRE25090207 to H.I.J.). The contents are solely the responsibility of the authors and do not necessarily represent the official views of the National Institutes of Health.

### REFERENCES

- Acs K, Luijsterburg MS, Ackermann L, Salomons FA, Hoppe T, Dantuma NP (2011). The AAA-ATPase VCP/p97 promotes 53BP1 recruitment by removing L3MBTL1 from DNA double-strand breaks. *Nat Struct Mol Biol* 18, 1345–1350.
- Alexa A, Varga J, Remenyi A (2010). Scaffolds are “active” regulators of signaling modules. *FEBS J* 277, 4376–4382.
- Anderson DJ, Le Moigne R, Djakovic S, Kumar B, Rice J, Wong S, Wang J, Yao B, Valle E, Kiss von Soly S, *et al.* (2015). Targeting the AAA ATPase p97 as an approach to treat cancer through disruption of protein homeostasis. *Cancer Cell* 28, 653–665.
- Bastola P, Neums L, Schoenen FJ, Chien J (2016). VCP inhibitors induce endoplasmic reticulum stress, cause cell cycle arrest, trigger caspase-mediated cell death and synergistically kill ovarian cancer cells in combination with salubrinal. *Mol Oncol* 10, 1559–1574.
- Blythe EE, Olson KC, Chau V, Deshaies RJ (2017). Ubiquitin- and ATP-dependent unfoldase activity of P97/VCP•NPLOC4•UFD1L is enhanced by a mutation that causes multisystem proteinopathy. *Proc Natl Acad Sci USA* 114, E4380–E4388.
- Chen SF, Wu CH, Lee YM, Tam K, Tsai YC, Liou JY, Shyue SK (2013). Caveolin-1 interacts with thd-1 and promotes ubiquitination and degradation of cyclooxygenase-2 via collaboration with p97 complex. *J Biol Chem* 288, 33462–33469.
- Cordeddu V, Di Schiavi E, Pennacchio LA, Ma'ayan A, Sarkozy A, Fodale V, Cecchetti S, Cardinale A, Martin J, Schackwitz W, *et al.* (2009). Mutation of SHOC2 promotes aberrant protein N-myristoylation and causes Noonan-like syndrome with loose anagen hair. *Nat Genet* 41, 1022–1026.
- Dantuma NP, Hoppe T (2012). Growing sphere of influence: Cdc48/p97 orchestrates ubiquitin-dependent extraction from chromatin. *Trends Cell Biol* 22, 483–491.
- de Araujo ME, Huber LA, Stasyk T (2008). Isolation of endocytic organelles by density gradient centrifugation. *Methods Mol Biol* 424, 317–331.
- Dhanasekaran DN, Kashef K, Lee CM, Xu H, Reddy EP (2007). Scaffold proteins of MAP-kinase modules. *Oncogene* 26, 3185–3202.
- Fernandez-Saiz V, Buchberger A (2010). Imbalances in p97 co-factor interactions in human proteinopathy. *EMBO Rep* 11, 479–485.
- Galperin E, Abdelmoti L, Sorkin A (2012). Shoc2 is targeted to late endosomes and required for Erk1/2 activation in EGF-stimulated cells. *PLoS One* 7, e36469.

- Gareau A, Rico C, Boerboom D, Nadeau ME (2018). In vitro efficacy of a first-generation valosin-containing protein inhibitor (CB-5083) against canine lymphoma. *Vet Comp Oncol* 16, 311–317.
- Gugliotta G, Sudo M, Cao Q, Lin DC, Sun H, Takao S, Le Moigne R, Rolfe M, Gery S, Muschen M, et al. (2017). Valosin-containing protein/p97 as a novel therapeutic target in acute lymphoblastic leukemia. *Neoplasia* 19, 750–761.
- Hannig V, Jeoung M, Jang ER, Phillips JA 3rd, Galperin E (2014). A novel SHOC2 variant in rasopathy. *Hum Mutat* 35, 1290–1294.
- Hanson PI, Whiteheart SW (2005). AAA+ proteins: have engine, will work. *Nat Rev Mol Cell Biol* 6, 519–529.
- Hanzelmann P, Schindelin H (2017). The interplay of cofactor interactions and post-translational modifications in the regulation of the AAA+ ATPase p97. *Front Mol Biosci* 4, 21.
- Heidelberger JB, Voigt A, Borisova ME, Petrosino G, Ruf S, Wagner SA, Beli P (2018). Proteomic profiling of VCP substrates links VCP to K6-linked ubiquitylation and c-Myc function. *EMBO Rep* 19, e44754.
- Jang ER, Galperin E (2016). The function of Shoc2: a scaffold and beyond. *Commun Integr Biol* 9, e1188241.
- Jang ER, Jang H, Shi P, Popa G, Jeoung M, Galperin E (2015). Spatial control of Shoc2-scaffold-mediated ERK1/2 signaling requires remodeling activity of the ATPase PSMC5. *J Cell Sci* 128, 4428–4441.
- Jang ER, Shi P, Bryant J, Chen J, Dukhande V, Gentry MS, Jang H, Jeoung M, Galperin E (2014). HUWE1 is a molecular link controlling RAF-1 activity supported by the Shoc2 scaffold. *Mol Cell Biol* 34, 3579–3593.
- Jang H, Oakley E, Forbes-Osborne M, Kesler MV, Norcross R, Morris AC, Galperin E (2019). Hematopoietic and neural crest defects in zebrafish shoc2 mutants: a novel vertebrate model for Noonan-like syndrome. *Hum Mol Genet* 28, 501–514.
- Jentsch S, Rumpf S (2007). Cdc48 (p97): a “molecular gearbox” in the ubiquitin pathway? *Trends Biochem Sci* 32, 6–11.
- Jeoung M, Abdelmohi L, Jang ER, Vander Kooi CW, Galperin E (2013). Functional integration of the conserved domains of Shoc2 scaffold. *PLoS One* 8, e66067.
- Kimonis VE, Fulchiero E, Vesa J, Watts G (2008a). VCP disease associated with myopathy, Paget disease of bone and frontotemporal dementia: review of a unique disorder. *Biochim Biophys Acta* 1782, 744–748.
- Kimonis VE, Mehta SG, Fulchiero EC, Thomasova D, Pasquali M, Boycott K, Neilan EG, Kartashov A, Forman MS, Tucker S, et al. (2008b). Clinical studies in familial VCP myopathy associated with Paget disease of bone and frontotemporal dementia. *Am J Med Genet Part A* 146A, 745–757.
- Lan B, Chai S, Wang P, Wang K (2017). VCP/p97/Cdc48, a linking of protein homeostasis and cancer therapy. *Curr Mol Med* 17, 608–618.
- Langeberg LK, Scott JD (2015). Signalling scaffolds and local organization of cellular behaviour. *Nat Rev Mol Cell Biol* 16, 232–244.
- Le Moigne R, Aftab BT, Djakovic S, Dhimolea E, Valle E, Murnane M, King EM, Soriano F, Menon MK, Wu ZY, et al. (2017). The p97 inhibitor CB-5083 is a unique disrupter of protein homeostasis in models of multiple myeloma. *Mol Cancer Ther* 16, 2375–2386.
- Lipson C, Alalouf G, Bajorek M, Rabinovich E, Atir-Lande A, Glickman M, Bar-Nun S (2008). A proteasomal ATPase contributes to dislocation of endoplasmic reticulum-associated degradation (ERAD) substrates. *J Biol Chem* 283, 7166–7175.
- Meerang M, Ritz D, Paliwal S, Garajova Z, Bosshard M, Mailand N, Janscak P, Hubscher U, Meyer H, Ramadan K (2011). The ubiquitin-selective segregase VCP/p97 orchestrates the response to DNA double-strand breaks. *Nat Cell Biol* 13, 1376–1382.
- Meyer H, Bug M, Bremer S (2012). Emerging functions of the VCP/p97 AAA-ATPase in the ubiquitin system. *Nat Cell Biol* 14, 117–123.
- Mountassif D, Fabre L, Zaid Y, Halawani D, Rouiller I (2015). Cryo-EM of the pathogenic VCP variant R155P reveals long-range conformational changes in the D2 ATPase ring. *Biochem Biophys Res Commun* 468, 636–641.
- Papadopoulos C, Meyer H (2017). Detection and clearance of damaged lysosomes by the endo-lysosomal damage response and lysophagy. *Curr Biol* 27, R1330–R1341.
- Piccirillo R, Goldberg AL (2012). The p97/VCP ATPase is critical in muscle atrophy and the accelerated degradation of muscle proteins. *EMBO J* 31, 3334–3350.
- Rodriguez-Viciano P, Oses-Prieto J, Burlingame A, Fried M, McCormick F (2006). A phosphatase holoenzyme comprised of Shoc2/Sur8 and the catalytic subunit of PP1 functions as an M-Ras effector to modulate Raf activity. *Mol Cell* 22, 217–230.
- Tang WK, Li D, Li CC, Esser L, Dai R, Guo L, Xia D (2010). A novel ATP-dependent conformation in p97 N-D1 fragment revealed by crystal structures of disease-related mutants. *EMBO J* 29, 2217–2229.
- van den Boom J, Meyer H (2018). VCP/p97-mediated unfolding as a principle in protein homeostasis and signaling. *Mol Cell* 69, 182–194.
- van den Boom J, Wolf M, Weimann L, Schulze N, Li F, Kaschani F, Riemer A, Zierhut C, Kaiser M, Iliakis G, et al. (2016). VCP/p97 extracts sterically trapped Ku70/80 rings from DNA in double-strand break repair. *Mol Cell* 64, 189–198.
- Vekaria PH, Home T, Weir S, Schoenen FJ, Rao R (2016). Targeting p97 to disrupt protein homeostasis in cancer. *Front Oncol* 6, 181.
- Watts GD, Thomasova D, Ramdeen SK, Fulchiero EC, Mehta SG, Drachman DA, Weihl CC, Jamrozik Z, Kwiecinski H, Kaminska A, Kimonis VE (2007). Novel VCP mutations in inclusion body myopathy associated with Paget disease of bone and frontotemporal dementia. *Clin Genet* 72, 420–426.
- Weihl CC, Pestronk A, Kimonis VE (2009). Valosin-containing protein disease: inclusion body myopathy with Paget’s disease of the bone and fronto-temporal dementia. *Neuromuscul Disord* 19, 308–315.
- Wojcik C, Yano M, DeMartino GN (2004). RNA interference of valosin-containing protein (VCP/p97) reveals multiple cellular roles linked to ubiquitin/proteasome-dependent proteolysis. *J Cell Sci* 117, 281–292.
- Ye Y, Tang WK, Zhang T, Xia D (2017). A mighty “protein extractor” of the cell: structure and function of the p97/CDC48 ATPase. *Front Mol Biosci* 4, 39.
- Yi J, Chen M, Wu X, Yang X, Xu T, Zhuang Y, Han M, Xu R (2010). Endothelial SUR-8 acts in an ERK-independent pathway during atrioventricular cushion development. *Dev Dyn* 239, 2005–2013.
- Zhou HJ, Wang J, Yao B, Wong S, Djakovic S, Kumar B, Rice J, Valle E, Soriano F, Menon MK, et al. (2015). Discovery of a first-in-class, potent, selective, and orally bioavailable inhibitor of the p97 AAA ATPase (CB-5083). *J Med Chem* 58, 9480–9497.